Exploring the limits to energy scaling and distant-target delivery of high-intensity midinfrared pulses

Paris Panagiotopoulos, Miroslav Kolesik, and Jerome V. Moloney

Phys. Rev. A **94**, 033852 — Published 28 September 2016

DOI: 10.1103/PhysRevA.94.033852

Exploring the limits to energy-scaling and distant-target delivery of high-intensity mid-infrared pulses

Paris Panagiotopoulos[1,2], Miroslav Kolesik[1,2], Jerome V. Moloney[1,2,3],
[1] College of Optical Sciences, University of Arizona, Tucson 85721-0094
[2] Arizona Center for Mathematical Sciences, University of Arizona, Tucson 85721-0094
[3] Department of Mathematics, University of Arizona, Tucson 85721-0094

We numerically investigate the scaling behavior of mid-infrared filaments at extremely high input energies. It is shown that given sufficient power, km-scale low-loss atmospheric filamentation is attainable by pre-chirping the pulse. Fully resolved four-dimensional ($xyzt$) simulations show that while in a spatially imperfect beam the modulation instability can lead to multiple hot spot formation, the individual filaments are still stabilized by the recently proposed mechanism that relies on the temporal walk-off of short-wavelength radiation.

I. INTRODUCTION

Worldwide efforts are actively underway to scale mid infrared (mid-IR) ultrashort laser pulses to supercritical powers capable of initiating and sustaining long range filamentation in the atmosphere (the critical power scales as λ^2) . Femtosecond duration sources are anticipated to operate within the $3.5-4.1$ μm atmospheric transparency window soon, delivering many tens to hundreds of millijoules. At even longer wavelengths of $9-11$ μm pulses with durations of hundreds of femtoseconds up to a few picoseconds are expected to deliver multiple joule energies. The use of mid-IR wavelengths for atmospheric applications is important, since even ground level turbulence is strongly mitigated at these longer wavelengths, as is well known for linear beams. As we shall see below a further advantage is that the nonlinear filament waists are typically much smaller than the inner scale of turbulence (scales as $\lambda^{6/5}$) at these longer wavelengths, further faciliating long range propagation. Finally, the major limitation to the latter in this regime, namley linear diffraction, is offset by filaments sustained over hundreds of meters and capable of transporting multiple terwatts of power.

Numerous theoretical and experimental works have recently investigated the properties of mid-IR filaments in gases. Bright coherent keV x-rays were generated in high pressure capillaries through filamentation of $\lambda = 4$ μm pulses [1]. The extremely broad spectral bandwidth that can be generated by mid-IR pulses offers the possibility of generating zeptosecond duration pulses, which was highlighted in Ref. [2]. The first experimental demonstration of a focused 3.9 μm, 200 GW filament in the atmosphere was demonstrated in [3]. Very recently it was shown that mid-IR pulses can be significantly compressed utilizing self phase modulation followed by dispersion compensation [4], a well established technique for $\sim$800 nm wavelengths. Moreover, strong-field physics is also moving towards the utilization of mid-IR lasers sources [5].

Previous theoretical work has demonstrated a new type of filamentation paradigm in the mid-IR where the physics are driven by the electric field rather than the field envelope. Here nonlinearity, although weak, dominates over an even weaker dispersion in transparent solids and gases. The end result is the formation of a carrier wave shock well before the onset of critical self-focusing. This results in the generation of a cascade of spectrally broad dispersive waves encompassing multiple harmonics [6]. Moreover, filaments formed in this regime are about ten times wider than their UV-to-near-IR counterparts, can transport much greater power/energy and propagate over tens of meters with minimal ionization losses [7]. Extensive numerical studies showed that this new regime of low-dispersion-high-nonlinearity can indeed be found in various materials, such as noble gases and single crystal diamond [8].

Key observations from our current study are that mid-IR filamentation should be extremely robust and scalable to multiple km ranges due primarily to cascades of carrier shock wave regularization events that limit achievable peak intensities, thereby signifcantly reducing ionization losses typical of IR USPs. While multiple filaments can form with very wide beams, their number is dramatically reduced, from hundreds with typical 100 μm waists, to just a few with 1-2 mm waists due to a significant scaling up of the underlying modulational instability growth wavelength.

II. NUMERICAL MODEL AND INPUT CONDITIONS

The numerical model used in the simulations is the unidirectional pulse propagation equation (UPPE). It is self evident that optical carrier shocks, which prevail here, cannot be captured by a nonlinear envelope model. We initially adopt a radial symmetry to facilate multiparameter studies. We later relax the radial symmetry assumption for two reasons, one to account for symmtery breaking multiple filamentation and the second less obvious one that artifical "rogue-wave-like" events observed in simulations downstream are often forced by such a symmetry restriction (see supplement in [7]). A detailed description of the numerical code can be found in [9].

The input wavepackets used in this work have a central wavelength of 4 μm, with durations varying from 24 fs up to (chirped) 350 fs at full width half maximum (FWHM), and beam waists that vary from 1.5 cm up to

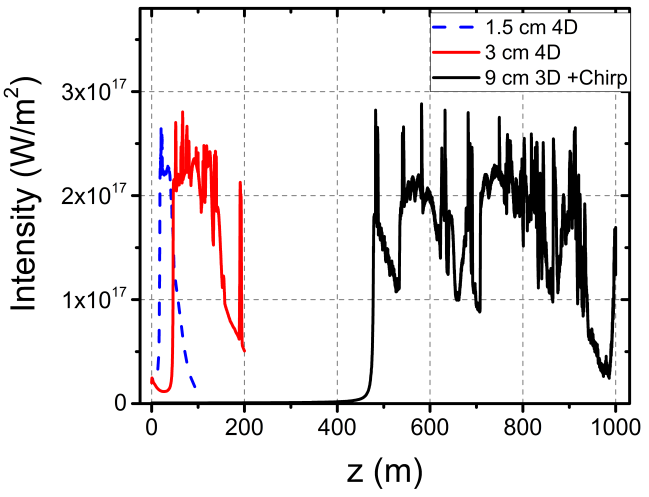

FIG. 1. (Color Online) Peak on-axis intensities vs propagation distance in three different pulses. Blue dashed line: 24 fs 1.5 cm input beam from [7], Red continuous line: 24 fs 3 cm beam simulated under assumption of axial symmetry over 200m. Black line: 350 fs chirped pulse with 9 cm beam waist simulated over 1 km propagation distance (with axial symmetry assumption).

9 cm at $1/e^2$ radius. The wavepackets propagate in dry air at 1 atm pressure. Dispersion of air is modeled using the Sellmeier equation [10], while the nonlinear refractive index associated with self-focusing is extrapolated from 800 nm based on [11], and the ionization potential of oxygen is 12.03 eV, as was the case in [7].

III. RESULTS

In Fig.1 we record the peak intensity of mid-IR filaments over a 1 km distance for three different pulses propagating in dry air. The blue dashed line represents the 24 fs 1.5 cm 177 mJ wavepacket studied in [3], forming a single filament of roughly 40 m in length. The red continuous line shows the scaling up in input energy to 0.8 Joule with the beam waist increased to 3 cm in order to avoid strong Kerr self-focusing in the early stages of propagation. The filament is now well over 100 m long, being clamped to similar intensity values as in the lower-energy case due to carrier shock walk-off which keeps ionization losses to a minimum.

In order to extend mid-IR filamentation even further, we applied negative pre-chirp to the input wave packet. The resulting pulse is 350 fs long at FWHM, with a chirp parameter of $c = -10$. At low power the given pulse would fully time-compress down to 38 fs at a distance of roughly 1 km due to atmospheric dispersion. The temporal compression would increase the peak intensity by a factor of 9. This well-established technique has proven very effective in extending the length and delaying the filament formation in the near-IR [12, 13]. While pre-chirping delays the onset of filamentation, it was necessary to increase the beam waist to 9 cm, in order keep the initial beam intensity low enough to prevent early self-focusing. Consequently, the input energy of this pulse is extremely high at 2.87 Joules.

The peak intensity vs z of the chirped 350 fs 9 cm wavepackets is depicted in Fig.1 as the black continuous line. The filament forms abruptly at $z = 477$ m and persists over a 460 m distance, while maintaining a stable $1-2$ mm beam waist after formation. The intensity profile is very similar to the lower energy cases, with multiple long lasting plateaus and occasional spikes every ~ 50 m. The temporal snapshots of the electric fields (not shown here) of both higher energy cases (red line: 0.8 J and black line: 2.87 J) show multiple walk-off events that extract energy out of the main pulse in the form of shock-seeded higher harmonics that propagate at slower speed. This process is visualized in the supplementary movie of the radial-temporal intensity profile vs propagation distance (see supplementary [14]). It shows the same mechanism found for the lower energy case (blue line: 177 mJ) recently studied in [7]. The overall energy losses over the 1 km propagation distance are $\sim 4\%$.

The spikes observed in the peak intensity every ~ 50 m in the 2.87 J case are local on-axis hot spots that briefly overcome the walk-off mechanism only to be arrested by ionization and plasma defocussing. These on-axis spikes are accentuated in radial symmetric spatial computational grids (see supplementary material in [7]) and lead to an artificial enhancement in ionization losses relative to full 4D simulations as we shall now show. In a previous work [7], we have shown that full 4D (xy: spatial dimensions, t, z) simulations can lead to notable differences compared to radially symmetric ones, especially for strongly perturbed input beams. Furthermore, by employing full 4D simulations we can investigate multi-filamentation sourced by strongly aberrated initial beams. Notably, even strong initial beam perturbations used in [7] did not result in a sustained modulation instability and multiple hotspot formation. The main reasons behind the resilience of mid-IR filaments concerning beam breakup is attributed to the walk-off mechanism, to an initialy smaller transverse beam waist and the scaling of modulation instability growth as the inverse of the wavelength (see supplementary material of [7]).

In order to investigate mid-IR multiple-filamentation in the atmosphere we simulated our highest energy case of chirped 350 fs - 9 cm - 2.87 J in four dimensions: two spatial dimensions, time, and propagation distance. To mimic a realistic wave packet we purposely added strong spatial random phase perturbations to the input beam profile in a similar fashion as in [7] (amplitude of 0.15 and a correlation length of 1 mm).

At this point we would like to note that simulating this 350 fs - 9 cm - 2.87 J wave packet in 4D with initial perturbations over a 1 km distance is an extremely demanding task. The simulation did run on our in-house SGI UV2000 super computer in parallel on 240 cores using ~ 3 TB of shared RAM. Computation time was 2 calendar months. The computational box dimensions used

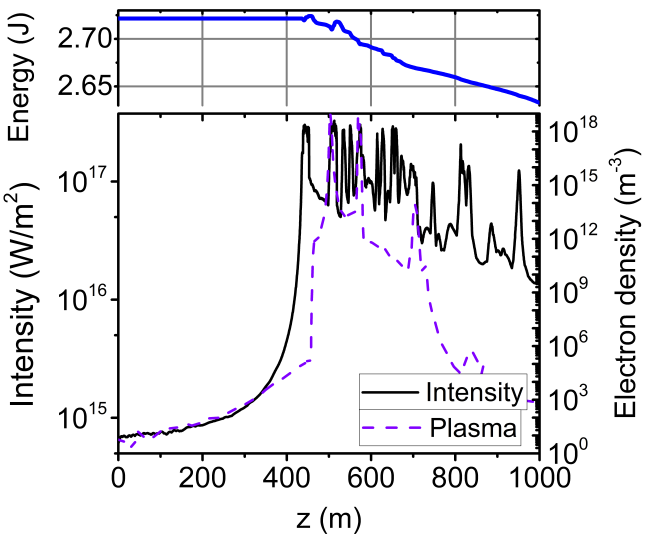

FIG. 2. (Color Online) Bottom: peak intensity (black continuous line) and integrated plasma density (magenta dashed line) vs propagation distance of a 350 fs chirped pulse with 9 cm initial beam waist containing initial perturbations. Top: Total approximate energy contained in the computational box vs propagation distance. Simulation in xyzt.

where: 20 cm × 20 cm × 3 ps × 1000 m with 2048 × 2048 × 4096 points respectively, resolving a total of 16.1 billion degrees of freedom for a single pulse snapshot and generating 2 TB of unprocessed data.

For all radial symmetric simulations shown in Fig.1, numerical convergence was ensured by gradually increasing resolution to the point where results remain unaffected. For the large 4D simulation described in the previous paragraph we use the highest resolution within our computational capabilities. While it was not possible to increase the resolution further, the given discretization does converge in radial symmetry. In addition the simulation results show only a few minor numerical artifacts as can be seen in Fig.2 and Fig.3, as well as in the supplementary movies online [15–17]. The energy of the wavepacket is calculated approximately by using a first order integration scheme, which is less accurate than then the simulation itself, but sufficient for qualitative observation.

Fig.2 shows the peak intensity (black continuous line), generated plasma density (magenta dashed line) and approximate total energy inside the computational box (blue line in the top inset) along propagation distance.The filament is formed at $z \simeq 440$ m and is sustained with occasional spikes throughout the rest of the propagation. The generated plasma density is very low and only reaches values over $10^{18}\ m^{-3}$ twice, which keeps the energy losses as low as $\sim 3.26\%$, delivering more than 2.6 J at the 1 km distant target. Note that bulk of the energy losses is due to the radiation leaving the computational box and being absorbed by the boundary (time, space and spectral domains), while a small portion is lost due to ionization.

As in the radially symmetric case, the main regularizing mechanism here is higher harmonic walk-off which continuously extracts energy out of the pulse in the temporal domain after the filament is formed. A movie of the evolution of the on-axis electric field and on-axis spectrum along propagation distance can be found in the supplementary material online [15, 16]. As before, there are occasional instances where ionization occurs, here at $z \simeq 500$ m and $z \simeq 550$ m, when the walk-off mechanism cannot effectively offset self-focusing. While mJ-level mid-IR filaments are mainly stabilized by higher harmonic walk-off, high energy multi-Joule filaments on the other hand may involve infrequent ionization events when walk-off is not strong enough.

Fig.3 shows snapshots of transverse xy-fluence profiles at fixed distances along the propagation path corresponding to the data in Fig.2. In the top left frame we can see xy-fluence of the beam after propagating 100 m in the atmosphere, with the initial perturbations clearly noticeable. The remaining frames from left to right along the top show the formation of the two distinct hotspots, most pronounced at $z \simeq 460$ m. Note the black square in the second graph indicates the zoomed-in axes used in the rest of the frames long the bottom row in Fig.3 in order to show more detail. The dynamics get more complex from this point on, with the beam forming multiple hotspots at seemingly random locations. As expected the individual filament widths and lengths are consistent with those for lower energies, i.e. ~ 1 mm wide and ~ 30 m long. Unlike traditional 800 nm multi-filaments that generate multiple plasma channels, mid-IR multi-filaments are extremely energy efficient because of very limited plasma generation resulting in $\sim 4\%$ of the total energy loss. A movie showing the evolution of the xy-fluence over the whole 1 km distance can be found in the supplementary file online [17].

IV. SUMMARY

In conclusion we have investigated the filamentation of mid-IR pulses in the atmosphere and the scaling to high input energies. By negatively pre-chirping the input wavepacket, we are able to predict that extremely long low loss filaments can reach km long distances. We have shown that the walk-off mechanism responsible for the stabilization of lower energy mid-IR filaments is still the main regularization mechanism when energy is scaled up to multi-Joule level. However, in extreme cases plasma generation does occasionally become necessary to arrest the collapse of the wavepacket. While mid-IR beams can also break up into multiple filaments, individual filament characteristic waists at 4 μm remains at 1-2 mm and these are more robust due to a slower modulational instability growth. We are currently aware of a large push to develop mid-IR ultra-short pulsed sources at tens to hundreds mJ at 4 μm and multi-Joule level ultra-short pulses at 10 μm making our results especially timely. We expect that properly engineered mid-IR filaments in the

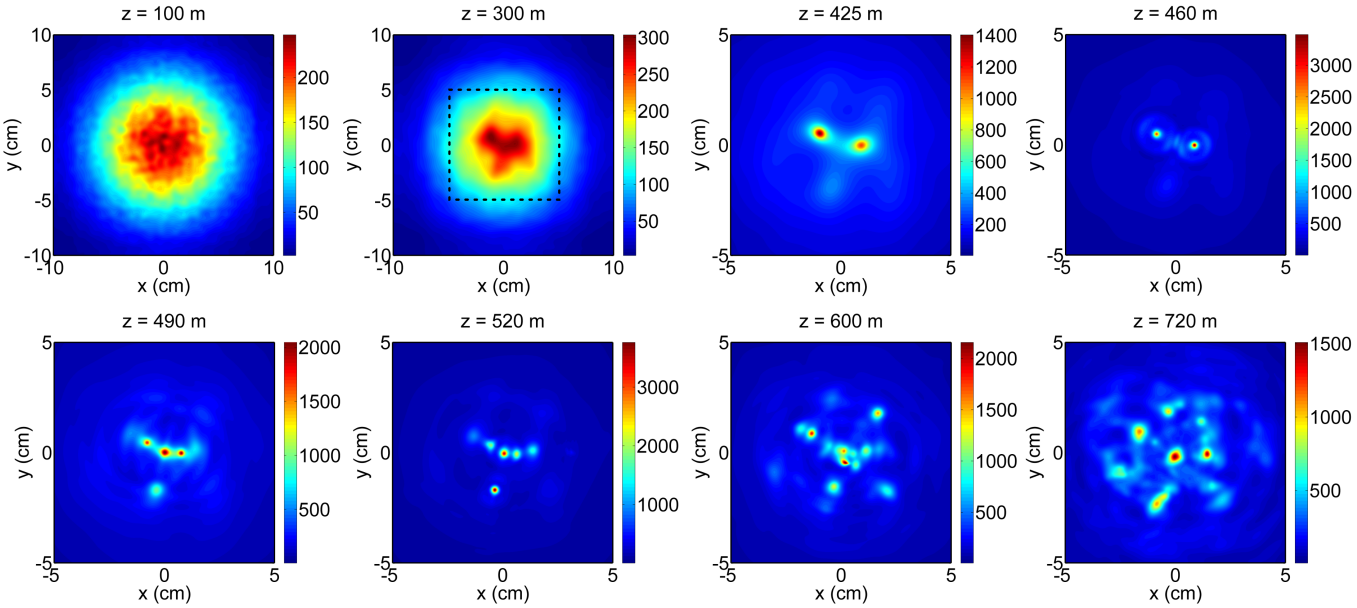

FIG. 3. (Color Online) Imperfect pulsed mid-IR beam breaking up in multiple filaments. XY crossection of fluence snapshots of the chirped 350 fs - 9 cm - 4 μ - 2.87 J wavepacket with initial perturbations shown at various position along propagation distance. The dashed square in the second subfigure of first line indicates the region showed in the consequent snapshots (10×10 cm). Simulation in xyzt. See supplementary movie online [17].

atmosphere to be scalable to even longer distances given enough power.

Acknowledgments: This work was supported by the following research grands: "Long Wavelength Electromagnetic Light Bullets Generated by a 10 μm CO_2 Ultrashort Pulsed Source AFOSR FA9550-15-1-0272, and "Carrier Based Long Wavelength Electromagnetic Light Bullets, Carrier Shock Initiated Exotic Waveforms and Extreme NLO Pulse Delivery to Targets, AFOSR FA9550-16-1-0088.

[1] C. Hernndez-Garca, J. A. Prez-Hernndez, T. Popmintchev, M. M. Murnane, H. C. Kapteyn, A. Jaron-Becker, A. Becker, and L. Plaja, "Zeptosecond High Harmonic keV X-Ray Waveforms Driven by Midinfrared Laser Pulses," Phys. Rev. Lett. **111**, 033002 (2013).

[2] T. Popmintchev, M.-C. Chen, D. Popmintchev, P. Arpin, S. Brown, S. Aliauskas, G. Andriukaitis, T. Baliunas, O. D. Mcke, A. Pugzlys, A. Baltuka, B. Shim, S. E. Schrauth, A. Gaeta, C. Hernndez-Garca, L. Plaja, A. Becker, A. Jaron-Becker, M. M. Murnane, and H. C. Kapteyn, "Bright Coherent Ultrahigh Harmonics in the keV X-ray Regime from Mid-Infrared Femtosecond Lasers," Science **336**, 1287-1291 (2012).

[3] A. V. Mitrofanov, A. A. Voronin, D. A. Sidorov-Biryukov, A. Pugzlys, E. A. Stepanov, G. Andriukaitis, T. Flory, S. Alisauskas, A. B. Fedotov, A. Baltuska, and A. M. Zheltikov, "Mid-infrared laser filaments in the atmosphere," Sci. Rep. **5** (2015).

[4] A. V. Mitrofanov, A. A. Voronin, D. A. Sidorov-Biryukov, S. I. Mitryukovsky, A. B. Fedotov, E. E. Serebryannikov, D. V. Meshchankin, V. Shumakova, S. Ališauskas, A. Pugžlys, V. Y. Panchenko, A. Baltuška, and A. M. Zheltikov, "Subterawatt few-cycle mid-infrared pulses from a single filament," Optica **3**, 299-302 (2016).

[5] B. Wolter, M. G. Pullen, M. Baudisch, M. Sclafani, M. Hemmer, A. Senftleben, C. D. Schroter, J. Ullrich, R. Moshammer, and J. Biegert, "Strong-Field Physics with Mid-IR Fields," Physical Review X **5**, 021034 (2015).

[6] P. Whalen, P. Panagiotopoulos, M. Kolesik, and J. V. Moloney, "Extreme carrier shocking of intense long-wavelength pulses," Phys. Rev. A **89**, 023850 (2014).

[7] P. Panagiotopoulos, P. Whalen, M. Kolesik, and J. V. Moloney, "Super high power mid-infrared femtosecond light bullet," Nat Photon **9**, 543-548 (2015).

[8] P. Panagiotopoulos, P. Whalen, M. Kolesik, and J. V. Moloney, "Carrier field shock formation of long-wavelength femtosecond pulses in single-crystal diamond and air," Journal of the Optical Society of America B **32**, 1718-1730 (2015).

[9] M. Kolesik, and J. V. Moloney, "Nonlinear optical pulse propagation simulation: From Maxwell's to unidirectional equations," Phys. Rev. E **70**, 036604 (2004).

[10] E. R. Peck and K. Reeder, "Dispersion of Air," J. Opt. Soc. Am. **62**, 958 (1972).

[11] J. Wahlstrand, Y. H. Cheng, and H. Milchberg, "Absolute measurement of the transient optical nonlinearity in N_2, O_2, N_2O, and Ar," Phys. Rev. A **85**, 043820 (2012).

[12] H. Wille, M. Rodriguez, J. Kasparian, D. Mondelain, J. Yu, A. Mysyrowicz, R. Sauerbrey, J. P. Wolf, and L. Woste, "Teramobile: A mobile femtosecond-terawatt laser and detection system," Eur. Phys. J. Appl. Phys. **20**, 183-190 (2002).

[13] P. Rairoux, H. Schillinger, S. Niedermeier, M. Rodriguez, F. Ronneberger, R. Sauerbrey, B. Stein, D. Waite, C. Wedekind, H. Wille, L. Wste, and C. Ziener, "Remote sensing of the atmosphere using ultrashort laser pulses," Appl. Phys. B **71**, 573-580 (2000).
[14] Movie 1km3DIrt
[15] Movie 1km4DField
[16] Movie 1km4DSpectrum
[17] Movie 1km4DFluence